CICE 2023 Rio de Janeiro - Brazil 11TH INTERNATIONAL CONFERENCE ON FRP COMPOSITES IN CIVIL ENGINEERING

# DESIGN OF FIBRE-POLYMER COMPOSITE STRUCTURES (CEN/TS 19101): ULS ANALYSIS OF A SPATIAL RETICULAR STRUCTURE

Salvatore Russo, Università IUAV di Venezia, Italy, russo@iuav.it
J. Toby Mottram, University of Warwick, United Kingdom, J.T.Mottram@warwick.ac.uk
Diego A. Talledo, Università IUAV di Venezia, Italy, diego.talledo@iuav.it
Michele Tondi, IN20 S.r.l., Italy, tondimichele@in20.eu

## ABSTRACT
Presented in this paper is a worked example to demonstrate the practical application of the CEN European Technical Specification CEN/TS 19101:2022 when designing a spatial reticular structure that has been constructed inside the Santa Maria Paganica church, Italy, following severe damaged by the 2009 L'Aquila earthquake. The example showcases the use of fibre-polymer composites to create a lightweight, resilient shelter that ensures the structural integrity and seismic safety over the time interval necessary for restoration of the damaged church. This worked example summarizes the structural analysis and ULS verification checks carried out to meet the requirements of CEN/TS 19101, thereby emphasizing its effectiveness in facilitating the design process to safeguard historic sites during restoration projects.

## KEYWORDS
CEN/TS 19101; Pultruded elements; Spatial reticular structure; ULS checks.

## INTRODUCTION
The Santa Maria Paganica church in L'Aquila, Italy, suffered significant damage during the devastating earthquake of 2009 (Russo 2012). It was rated 6.3 on the moment magnitude scale. In the aftermath of the disaster, the church's integrity was severely compromised, as seen in Figure 1, leaving it vulnerable to further deterioration from environmental actions such as from snow, rain, and other adverse weather conditions. To protect this cultural heritage site until the restoration works could happen there was an urgent need for a robust and lightweight shelter that provided temporary cover to prevent additional damage the church's fabric. The shelter of fibre-polymer composite materials for the Santa Maria Paganica church was executed in 2011.

In recent years, the field of structural engineering has witnessed significant advancements in the use of fibre-polymer composites for constructing resilient and durable structures. These composite materials, comprising high-performance fibres embedded in a thermosetting polymer matrix, offer a unique combination of strength, stiffness, and lightweight characteristics, making them an ideal choice for new-build structural applications, and, when needed, for the retrofitting intervention of historical buildings.

In November 2022, the European Committee for Standardization (CEN) published the Technical Specification CEN/TS 19101:2022, "Design of Fibre-Polymer Composite Structures", which is a key milestone towards the widespread application of fibre-reinforced-polymer materials in civil engineering structures. This Technical Specification aims at providing clear guidance on how to design structures, taking account of various factors, such as short and long-term material properties, loadings, and the European limit state design methodologies. Throughout the rest of the paper the abbreviation TS will be used for CEN/TS 19101:2022. The TS is concerned with the design requirements for resistance, serviceability, durability and fire resistance. In the TS, fibre-polymer composite materials are referred to as composite materials or as composites. The TS describes a general basis for the design of composite structures composed of (i) composite members, or (ii) combinations of composite members and members of other materials (hybrid-composite structures), and (iii) the joints between these members. Accompanying the TS will be a set of 16 Worked Examples together with a Commentary of 1000 pages having background information for provenance to the design procedures, etc. Funds are being sourced to permit these key documents to be published open access. The Commentary functions as a technical audit trail for the criteria underpinning decisions made when drafting the TS and the Worked Examples will support designers carrying out trial designs that will generate feedback comments to support the Stage 3 transformation of the TS into the formal recognised Eurocode standard.

The practical application of the TS with real-world scenarios, such as for post-earthquake protective shelter design (Russo 2012), remains an area that requires further exploration. Therefore, the purpose of one of the 16 Worked Examples, which is summarized herein, is for a case study illustrating the application of the TS for the design of a spatial reticular structure (see Figures 1 to 3), serving as a protective shelter to the masonry fabric of the Santa Maria Paganica church. Through comprehensive structural analysis and design calculations for verification of ULS modes of failure, this study demonstrates how composites can be employed to create a lightweight and resilient shelter, effectively safeguarding the church from environmental actions during the waiting period before restoration works commence. It is noted that the shelter was designed shortly after the 2009 earthquake using engineering expertise and no 'standard' design verification procedures, and so another outcome from preparing this worked example is to show that the composite shelter always had a safe and reliable structural design.

By showcasing the practical implementation of the TS, the contents of this paper contribute to the growing body of knowledge and understanding in the field of composite structures, and offers insights into the design process, considerations, and challenges involved in creating protective shelters for historical structures. Furthermore, the worked example emphasizes the importance of sustainable and durable solutions in post-earthquake reconstruction, ensuring the long-term preservation of cultural heritage sites.

The paper is structured as follows: after this brief introduction, the framed structure itself is briefly described for structural analysis and design, by presenting the geometrical and material characteristics, together with the finite element model for global structural analysis; next reported are the results, in terms of internal member forces from applying the seven load cases; followed by an introduction to three of the main ULS verifications; and, ending with the reporting of key conclusions.

## THE ANALYSED STRUCTURE

Seen in Figure 1 is the skeletal frame structure to be analysed for the effect of actions (EN 1990; 2002) from the design load cases. It is one of the two composite structures that has protected the earthquake damaged church of Santa Maria Paganica. To be able to accommodate the necessary restoration activities this shelter unit is 27 m long, 17.3 m wide and 32 m high. Erection took place during 2011. The frame has members of composite profiles produced by the pultrusion processing method. The frame consists of primary built-up members constructed of four C-profiles connected by means of stainless-steel bolting. Bolted structural joints between the primary members use gusset plates produced using the bag-moulded composite processing method. Both composite materials have glass fibre reinforcement. To make the frame structure stable the built-up column members are embedded at their bases into lightly reinforced concrete pedestals standing directly onto the church's floor. Photographic images in Figure 1a and 1b show views of the installed structure and that the church's roof and parts of the masonry wall's had collapsed. To protect its interior from the weather environment a geotextile fabric covering is placed over the composite structure.

The overall structure consists of different types of built-up members, as follows (Russo, 2012):

- four C-profiles for column and main truss members;
- two L-profiles for secondary truss elements;
- different types of two C-profiles for roof members.

The geometrical properties of the sections whose design verifications are presented later will be detailed in the sub-section "Cross-sectional geometrical properties".

a)

b)

Figure 1: View of the fibre-polymer composite structure that protects the earthquake damaged Santa Maria Paganica church: a) general view of the partially collapsed church with top of composite structure; b) view of the spatial frame structure looking up at its roof

**Finite element model for structural analysis**

A SAP2000 3D beam model was created to determine by finite element analyses the member forces and displacements when the frame structure is subjected to the design load cases. The structural analysis was linear elastic with the small displacement assumption. Figure 2 shows an isometric view of the created 3D model; at the bottom-left node of the model is, in cyan colour, the reference global coordinate system, with the y-axis in the longitudinal direction of the structure (27 m), the x-axis being aligned with the transverse direction (17.3 m) and the z-axis directed vertically upwards (32 m). Figure 3 shows a plan view of the repeating plane frame (in the x-z plane) that is repeated 10 times, or every 3 m, in the longitudinal x-direction. The locations of two members labelled Element 1 (is a column member) and 2 (is a roof member) are shown in this figure.

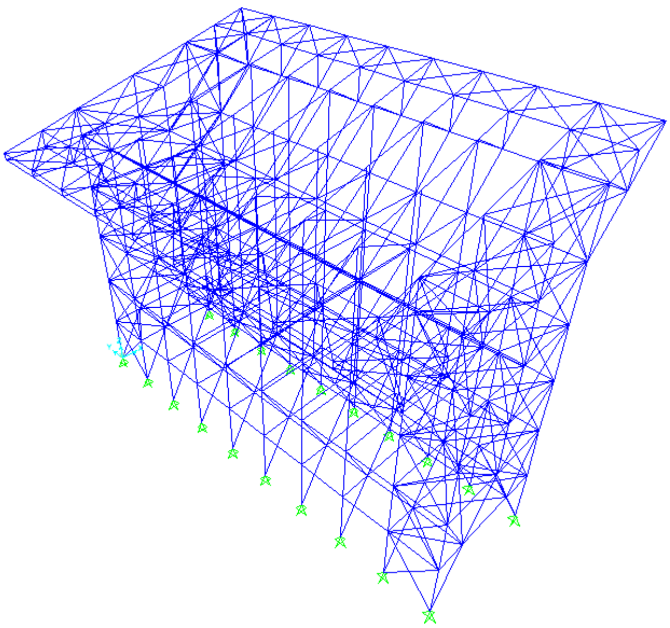

Figure 2: Isometric view of the 3D SAP2000 model of the framed structure for structural analysis

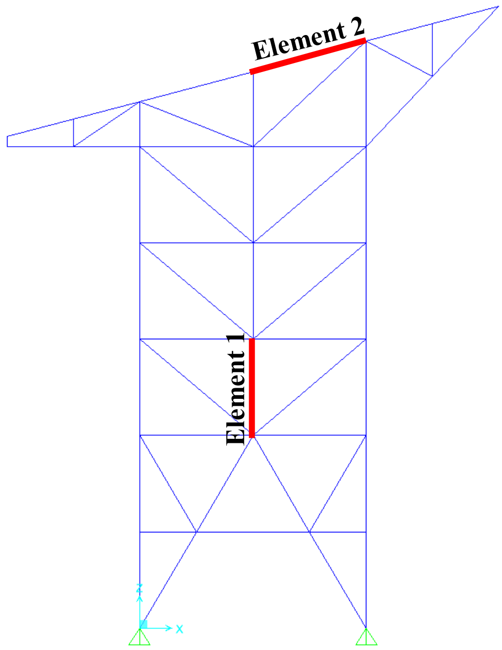


Figure 3: 2D view in the *x*-*z* plane of the repeating plane frame with labelling of the two elements (members) whose ULS verifications are presented in this paper

**Cross-sectional geometrical properties**

Figure 4 shows the cross-section, at a section having five M10 connecting bolts, for the first type of built-up member made of four C-profiles sized 152×46×9.5 mm, which is the cross-section for column Element 1. At the centre of the cross-section is a gusset plates. The local Cartesian co-ordinate axis system for the member has the cross-section in the y-z plane with the x-direction along the member's length. The roof Element 2 has a different cross-section that is constructed from two C-profiles of size 203×55×9 mm. Table 1 summarizes, with the symbols used in the worked example, the cross-sectional geometrical properties for Elements 1 and 2. Because the drilled holes for bolting, as seen in the figure, are considered in the ULS verification checks the net-section properties are used, when appropriate to do so.

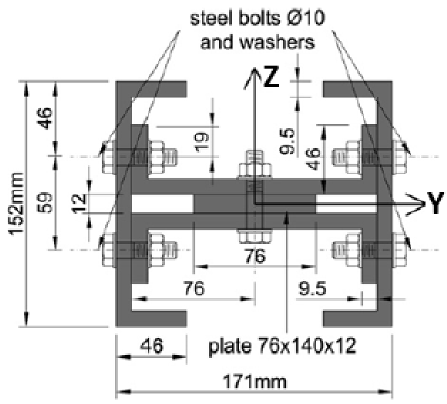


Figure 4: Built-up cross-section composed of four C-profiles (Russo, 2012)

Table 1: Cross-section geometrical properties for built-up members labelled Elements 1 and 2

| Property | Units | Element number | |
|---|---|---|---|
| | | 1 | 2 |
| Height of C-profile ($h$) | mm | 152.0 | 203,0 |
| Width of C-profile ($b$) | mm | 46.0 | 55,0 |
| Flange thickness ($t_f$) | mm | 9.5 | 9.0 |
| Web thickness ($t_w$) | mm | 9.5 | 9.0 |
| Area of built-up section ($A$) | $mm^2$ | 8550 | 5310 |
| Net area of built-up section ($A_{net}$) | $mm^2$ | 7505 | 4860 |
| Major-axis second moment of area of built-up section ($I_y$) | $mm^4$ | $3.24 \cdot 10^7$ | $2.814 \cdot 10^7$ |
| Net Major-axis second moment of area of built-up section ($I_{y,net}$) | $mm^4$ | - | $2.768 \cdot 10^7$ |
| Minor-axis second moment of area of built-up section ($I_z$) | $mm^4$ | $1.470 \cdot 10^7$ | $3.111 \cdot 10^6$ |
| Net Minor-axis second moment of area of built-up section ($I_{z,net}$) | $mm^4$ | - | $3.052 \cdot 10^6$ |
| Major-axis elastic modulus of built-up section ($W_y$) | $mm^3$ | $4.240 \cdot 10^5$ | $2.772 \cdot 10^5$ |
| Net major-axis elastic modulus of built-up section ($W_{y,net}$) | $mm^3$ | $4.240 \cdot 10^5$ | $2.723 \cdot 10^5$ |
| Minor-axis elastic modulus of built-up section ($W_z$) | $mm^3$ | $1.934 \cdot 10^5$ | $5.100 \cdot 10^4$ |
| Net minor-axis elastic modulus of built-up section ($W_{z,net}$) | $mm^3$ | $4.240 \cdot 10^5$ | $5.003 \cdot 10^4$ |
| Shear area of built-up section ($A_v$) | $mm^2$ | 2888 | 3654 |
| Net shear area of built-up section ($A_{v,net}$) | $mm^2$ | 2679 | 3150 |
| Major-axis radius of gyration of built-up section ($i_y$) | mm | 65.1 | 72.8 |
| Minor-axis radius of gyration of built-up section ($i_z$) | mm | 41.5 | 24.2 |
| Length of member ($L$) | mm | 3400 | 5100 |
| Major-axis slenderness ($\lambda_y$) | - | 52.2 | 70.2 |
| Minor-axis slenderness ($\lambda_z$) | - | 81.9 | 211.2 |

**Material properties**

Mean and characteristic values of key mechanical properties of the pultruded material were determined from test results based on 10 nominal identical coupon specimens per batch. The pultruded profiles have fibre reinforcement consisting of layers of E-glass rovings and woven cross-ply mats, which are embedded in a polymer matrix based on a vinylester resin (Russo 2012). The overall volume fraction of fibres is 40% giving a profile density ($\gamma_p$) of 17.5 kN/m$^3$. Listed in the twelve rows of Table 2 are the required mean and characteristic values of the material properties adopted in design, along with their material partial factors and conversion factors. There is not space in this paper to give details on how to establish the values for $\gamma_m$ and $\eta_c$, needless-to-say both the TS's Commentary and worked examples develops the necessary information that designers need to know.

Other relevant design parameters for structural analyses and the ULS design verifications are:

- Service temperature: $T_s$ = 20°C;
- Glass transition temperature of the pultruded materials: $T_g$ = 100°C;
- Exposure class: I (refer to sub-clause 4.4.7.3 in the TS).

Table 2: Mean, $X_m$, and characteristic, $X_k$, values of material properties for the pultruded profiles along with their material partial factors and conversion factors

| Property | Units | $X_m$ | $X_k$ | $\gamma_m$ | $\eta_c$ |
|---|---|---|---|---|---|
| | | [MPa]/[-] | [MPa]/[-] | [-] | [-] |
| $E_{x,c}$ | MPa | 23000 | 20665 | 1.09 | 1.00 |
| $E_{x,t}$ | MPa | 23000 | 20665 | 1.09 | 1.00 |
| $E_{y,c}$ | MPa | 8500 | 6249 | 1.29 | 1.00 |
| $E_{y,t}$ | MPa | 8500 | 6249 | 1.29 | 1.00 |
| $\nu_{xy}$ | - | 0.23 | 0.18 | 1.22 | 1.00 |
| $\nu_{yx}$ | - | 0.09 | 0.07 | 1.22 | 1.00 |
| $f_{x,c}$ | MPa | 350 | 318 | 1.09 | 1.00 |
| $f_{x,t}$ | MPa | 350 | 318 | 1.09 | 1.00 |
| $f_{y,c}$ | MPa | 70.0 | 55.2 | 1.22 | 1.00 |
| $f_{y,t}$ | MPa | 70.0 | 55.2 | 1.22 | 1.00 |
| $G_{xy}$ | MPa | 3000 | 2368 | 1.22 | 1.00 |
| $f_{xy,v}$ | MPa | 61.0 | 57.0 | 1.07 | 1.00 |

## PERFORMED STRUCTURAL ANALYSES

In this section, there is a brief report leading to the results from the structural analyses performed using the finite element modelling approach introduced above.

### Load cases and combinations

The only permanent action in the design load cases is from the weight of the of profiles, having $\gamma_p = 17.5\ \mathrm{kN/m^3}$. The weights of, gusset plates, steel bolting and the fabric covering for weather protection are neglected. More generally, it could be expected that corrugated sheets would be used for the roofing in the medium to long-term. The set of uniformly distributed loads (with characteristic values) applied at roof level are self-weight and other permanent loads ($g_k$) at $0.7\ \mathrm{kN/m^2}$ and snow load ($q_{s,k}$) at $3.2\ \mathrm{kN/m^2}$. Accounting for the spacing distance of 3.0 m between the plane frames (see Figures 2 and 3) these uniformly distributed loads become self-weight and other permanent loads ($g_k$) at $2.1\ \mathrm{kN/m}$ and snow load ($q_{s,k}$) at $9.6\ \mathrm{kN/m}$. The snow load was determined in accordance with EN 1991-1-3:2003 and the National Annex for Italy. The wind loads were computed, for the required wind directions, in accordance with EN 1991-1-4:2005 and the National Annex for Italy. All the relevant load combinations in EN 1990:2002 have been considered for ULS verification checks.

### Frame forces and moments

The effect of actions for the seven load cases were computed using SAP 2000 analyses. Figure 5 and 6 presented, respectively, numerical results in terms of axial force bending moment distribution envelopes obtained from combining the load combination cases. The design values in Figure 5 for axial forces are given by blue coloured lines for tension and red coloured lines for compression. Similarly, the design values in Figure 6 for the bending moments are presented. These effects of actions are displayed on the plane frame to show which members have the highest internal forces and moments; which includes Elements 1 and 2. From the bending moment distributions plotted in Figure 6 it is observed that, except for the continuous roof beam, the joints in rest of the frame are assumed to be nominal pinned, so at the joints the moment is zero (i.e. there are truss elements).

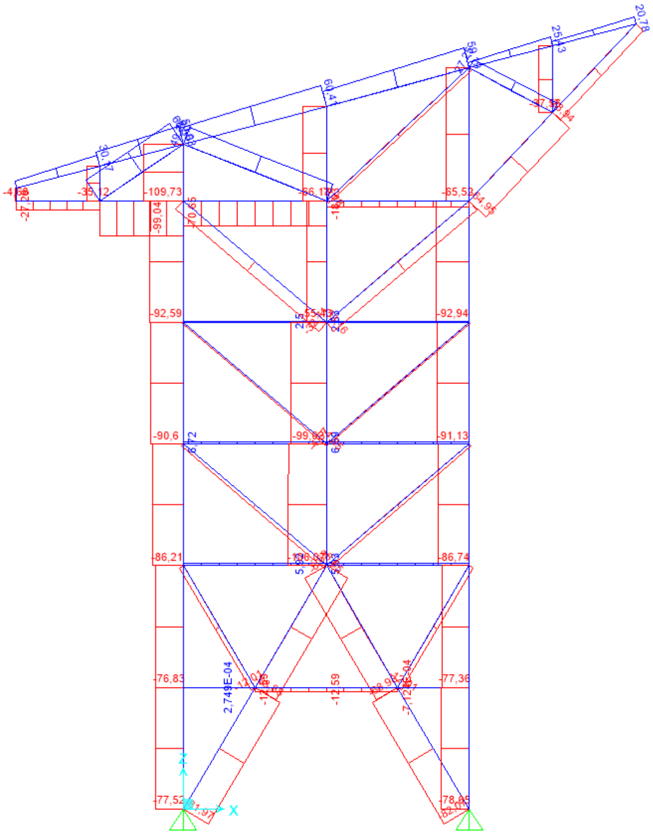

Figure 5: Envelope of design member axial force distributions [kN]

The design values for the maximum axial force, $N_{Ed}$, and maximum moment, $M_{Ed}$, in Elements 1 and 2 are summarized in Table 3 in terms of ULS design verifications for Element 1 of axial compression and of combined axial tension and bending moment and the ULS design verification for Element 2 of creep rupture.

Table 3: Maximum values of internal forces for design verification

| Internal force(s) for design verification | Element number (see Figure 3) | Axial force $N_{Ed}$ [kN] | Bending moment $M_{Ed}$ [kNm] |
|---|---|---|---|
| Axial compression | Element 1 | -106.1 | - |
| Axial tension/bending moment | Element 2 | 43.0 | 23.0 |
| Creep rupture | Element 2 | - | 0.4 |

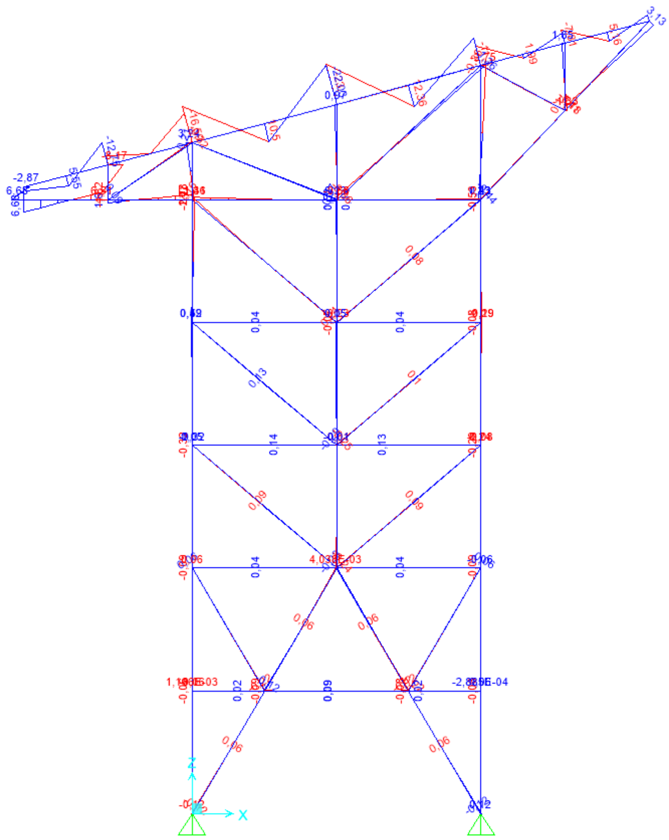

Figure 6: Envelope of design member bending moment distributions [kNm]

**ULS VERIFICATION CHECKS**

In the following sub-sections, we provide a flavour of the ULS verification checks that are presented in the Worked Example. The three sets of design calculations are for the two critical members (Elements 1 and 2) labelled in Figure 3, having the geometrical properties summarized in Table 1 and the adopted material properties listed in Table 2. The specific design checks are listed in the first column of Table 3. The partial factor for resistance models, $\gamma_{\mathrm{Rd}}$, for five different ULS failure modes of profiles and laminates, taken directly from the TS are reported in Table 4.

Table 4: Partial factors for resistance models

| Material failure | Global buckling | | | Local buckling |
|---|---|---|---|---|
| | Flexural | Lateral-torsional | Flexural-torsional | |
| 1.40 | 1.30 | 1.30 | 1.55 | 1.30 |

**Axial compression**

The first design verification is with Element 1 and is for axial compression, with $N_{\mathrm{Ed}}$ = -106.1kN, comprising checks for the ULS modes of failure of section crushing, and local or flexural (elastic) buckling. This ULS verification is for the first type of built-up cross-section using four C-profiles (see Figure 4) shall, in accordance with the TS, satisfy:

$$N_{\mathrm{c,Ed}} \leq N_{\mathrm{c,Rd}}; \quad \text{i.e.,} \ \frac{N_{\mathrm{c,Ed}}}{N_{\mathrm{c,Rd}}} \leq 1.0 \qquad \text{Eq. 1}$$

$N_{\mathrm{c,Rd}}$ is the design value of the compressive resistance in the longitudinal x-direction of the member, which is given by:

$$N_{\mathrm{c,Rd}} = \min\{N_{\mathrm{c,Rd1}}; N_{\mathrm{c,Rd2}}\} \qquad \text{Eq. 2}$$

where $N_{\mathrm{c,Rd1}}$ is the design value of the compressive resistance to crushing the cross-section, and $N_{\mathrm{c,Rd2}}$ is the compressive resistance to global buckling of the member or local buckling of the cross-section. $N_{\mathrm{c,Rd1}}$ for cross-sections with circular openings (bolt holes) and $A_{\mathrm{net}} > 0.6A$ is given by:

$$N_{\mathrm{c,Rd1}} = \frac{\eta_{\mathrm{c}}}{\gamma_{\mathrm{m}} \cdot \gamma_{\mathrm{Rd}}} \cdot 0.7 \cdot A_{\mathrm{net}} \cdot f_{\mathrm{x,c,k}} \qquad \text{Eq. 3}$$

Material partial factor, $\gamma_{\mathrm{m}}$, and the total conversion factor, $\eta_c$, for $f_{\mathrm{x,c,k}}$ = 318 MPa from Table 2, are equal to $\gamma_{\mathrm{m}} = 1.09$ and $\eta_{\mathrm{c}} = 1.0$. From Table 4 the partial factor for the resistance model, $\gamma_{\mathrm{Rd}}$, is equal to 1.40 for verification of material failure, which for a compression action is crushing. The application of Eq. 3 leads to a value of $N_{\mathrm{c,Rd1}} = 1093$ kN, which is a compression axial force.

$N_{\mathrm{c,Rd2}}$ for buckling failure of a doubly symmetric cross-section profile is given by:

$$N_{\mathrm{c,Rd2}} = \chi_E \cdot N_{\mathrm{cr,Rd}} \qquad \text{Eq. 4}$$

where $\chi_E$ and $N_{\mathrm{cr,Rd}}$ are, respectively, the reduction factor to take into account the interaction between local and flexural buckling, and the design value of the compressive resistance to local buckling. It is worth noting that the built-up cross-section (see Figure 4) was designed to avoid, or at least to minimise the likelihood, that the governing ULS mode of failure is local buckling (Russo, 2015). Therefore, $N_{\mathrm{cr,Rd}}$ in Eq. 4 is equal to the strength $N_{\mathrm{c,Rd1}}$ previously defined. The interaction factor $\chi_E$ is defined in accordance with the TS by:

$$\chi_E = \frac{1}{c_{\mathrm{E}} \cdot \lambda_{\mathrm{E}}^2} \cdot \left( \Phi_{\mathrm{E}} - \sqrt{\Phi_{\mathrm{E}}^2 - 0{,}65 \cdot \lambda_{\mathrm{E}}^2} \right), \text{ with } \chi_{\mathrm{E}} \leq 1{,}0 \qquad \text{Eq. 5}$$

where $c_{\mathrm{E}}$ is an empirical constant equal to 0.65, $\Phi_{\mathrm{E}}$ is an auxiliary variable equal to $(1 + \lambda_E^2)/2$ an $\lambda_E$ is slenderness of the member (Element 1) for the interaction between local and flexural buckling computed from:

$$\lambda_{\mathrm{E}} = \sqrt{\frac{N_{\mathrm{cr,Rd}}}{N_{\mathrm{E,Rd}}}} \qquad \text{Eq. 6}$$

where $N_{\mathrm{E,Rd}}$ is the design value of the flexural buckling strength of the profile, given by:

$$N_{\mathrm{E,Rd}} = \frac{1}{\gamma_{\mathrm{m}} \cdot \gamma_{\mathrm{Rd}}} \cdot A \cdot f_{\mathrm{E,k}} \cdot \chi_{\mathrm{E,shear}} \qquad \text{Eq. 7}$$

where $\gamma_{\mathrm{Rd}}$ is the partial factor for the resistance model and is 1.30 from Table 4. $\chi_{\mathrm{E,shear}}$ is a reduction factor accounting for the influence of shear deformability and with $G_{\mathrm{xy,k}} \approx 2400$ MPa its value is 0.96. $f_{\mathrm{E,k}}$ is the characteristic value of critical flexural buckling stress (disregarding the influence of shear deformability), and is given by the modified Euler formula:

$$f_{\mathrm{E,k}} = \frac{\pi^2 \cdot \eta_{\mathrm{c}} \cdot E_{\mathrm{x,c,k}}}{\left(\frac{k \cdot L}{i}\right)^2} \qquad \text{Eq. 8}$$

where $i$ is the radius of gyration about the relevant axis, which for minor axis flexural buckling is the minor radius of gyration, $i_z = 41.5$ mm and where the length of member $L = 3440$ mm are taken from the seventeen and eighteen rows in Table 1. $\eta_c = 1.0$ for the conversion factor associted with characterisitc value of the axial compressice modulus, $E_{x,\mathrm{c,k}}$, which is 20665 MPa from the first row in Table 2. In the TS mean values for elastic moduli are no used to determine buckling rsistances. $k$ is the effective length parameter to take into account the restraining effects of end supports; because the joints at the member's ends are assumed to be nominally pinned, $k = 1.0$, which ensures the value of $f_{\mathrm{E,k}}$ is the lowest it can take.

Applying Eq. 8, $f_{\mathrm{E,k}} = 30.4$ MPa and from Eq. 7, $N_{\mathrm{E,Rd}} = 176\ kN$. The slenderness of the profile $\lambda_{\mathrm{E}}$ is equal to 2.49 and thereby by Eq. 5 the reduction factor $\chi_E$ is equal to 0.15. This means that the axial compression strength of the profile owing to flexural buckling is reduced to 15% of the axial compressive strength, therby givieng compressive axial force $N_{\mathrm{c,Rd2}} = -164$ kN. The ULS check of Eq. 1 is therefore satisfied, being $N_{c,Ed}/N_{c,Rd} = -102/-164 = 0.65, < 1.0$.

**Combination of axial tension and bending**

The second verification is with Element 2 and is for combined axial tension and bending moment (about the major principal axis) with $N_{Ed}$ = 43.0 kN and $M_{Ed}$ = 23.0 kNm, comprising a resistance check for buckling interaction. This ULS design check is for the second type of built-up cross-section using two C-profiles (of size 203×55×9 mm), which shall, in accordance with the TS, satisfy:

$$\frac{N_{\text{t,Ed}}}{N_{\text{t,Rd}}} + \frac{M_{\text{Ed}}}{M_{\text{Rd1}}} \leq 1.0 \qquad \text{Eq. 9}$$

In Eq. 9, $N_{\text{t,Rd}}$ is the design value of the tensile resistance in the longitudinal x-direction of the member and $M_{\text{Rd1}}$ is the design value of the bending moment resistance to material (flange tensile/compressive) failure of the cross-section (about the major-axis). The design value for tensile resistance is, in accordance with the TS, given by:

$$N_{\text{t,Rd}} = \frac{\eta_{\text{c}}}{\gamma_{\text{m}} \cdot \gamma_{\text{Rd}}} \cdot 0.7 \cdot A_{\text{net}} \cdot f_{\text{x,t,k}} \qquad \text{Eq. 10}$$

The material partial factor, $\gamma_{\text{m}}$, and the conversion factor, $\eta_{\text{c}}$, for the characteristic tensile strength $f_{x,t,k}$ = 318 MPa from the eighth row in Table 2 is $\gamma_{\text{m}} = 1.09$ and $\eta_c = 1.0$. The partial factor for the resistance model, $\gamma_{\text{Rd}}$, from Table 4 is equal to 1.40 for verification of material failure as the ULS failure mode. Using Eq. 10 the calculated value of $N_{\text{t,Rd}} = 700$ kN.

The design value of the bending moment resistance to material is, in accordance with the TS, given by:

$$M_{\text{Rd1}} = 0.7 \cdot W_{\text{net}} \cdot \min\left\{\frac{\eta_c}{\gamma_{\text{m}} \cdot \gamma_{\text{Rd}}} \cdot f_{\text{x,t,k}}; \frac{\eta_c}{\gamma_{\text{m}} \cdot \gamma_{\text{Rd}}} \cdot f_{\text{x,c,k}}\right\} \qquad \text{Eq. 11}$$

The material partial factor, $\gamma_{\text{m}}$, and the nominal conversion factor, $\eta_c$, for the characteristic compressive strength $f_{\text{x,c,k}}$ = 318 MPa from the seventh row in in Table 2, is also $\gamma_{\text{m}} = 1.09$ and $\eta_{\text{c}} = 1.0$. From Eq. 11 the bending moment resistance of the cross-section, $M_{\text{Rd1}}$, is calculated to be 39.7 kNm.

The ULS verification check by Eq. 9 is satisfied, with $\frac{N_{\text{t,Ed}}}{N_{\text{t,Rd}}} + \frac{M_{\text{Ed}}}{M_{\text{Rd1}}} = \frac{43}{700} + \frac{23.0}{39.7} = 0.64$, < 1.0.

**Creep rupture**

*Tensile induced creep rupture*

The first part of the third ULS verification check is with Element 2 for the maximum sustained tensile stress owing to the long-term mode of failure being creep rupture. For this specific ULS the load case is defined by the quasi-permanent combinations of actions. In accordance with the TS, design against creep rupture shall satisfy:

$$\sigma_{\text{t,creep,Ed}} \leq \sigma_{\text{t,creep,Rd}}; \text{ i.e., } \frac{\sigma_{\text{t,creep,Ed}}}{\sigma_{\text{t,creep,Rd}}} \leq 1.0 \qquad \text{Eq. 12}$$

where $\sigma_{\text{t,creep,Rd}}$ is the design value of the tensile stress limit for creep rupture, and is determined using the following formula:

$$\sigma_{\text{t,creep,Rd}} = \frac{\eta_c}{\gamma_{\text{M,creep}}} \cdot k_{\text{t,creep}} \cdot f_{\text{i,t,k}} \qquad \text{Eq. 13}$$

The partial factor for creep rupture, $\gamma_{\text{M,creep}}$, takes a value of 1.5. The nominal conversion factor, $\eta_c$, corresponds to $f_{i,\text{t,k}} = f_{\text{x,t,k}}$, is equal to 1.0. The characteristic value of the tensile strength of the composite material in the pultrusion direction is $f_{\text{x,t,k}} = 318$ MPa (refer to eighth row in Table 2). The strength reduction factor for tensile creep rupture, $k_{\text{t,creep}}$, takes a value of 0.4. This value is for a constant stress period of 50 years. It is also specific to the composite material having continuous unidirectional glass fibre reinforcement, which the pultruded C-profiles satisfy. The application of Eq. 13 leads to a value of $\sigma_{\text{t,creep,Rd}} = 84.8$ MPa.

$\sigma_{\text{t,creep,Ed}}$ is the design value of the maximum sustained tensile stress caused by the quasi-permanent combination of actions and, in accordance with the TS, is determined from:

$$\sigma_{\text{t,creep,Ed}} = \frac{M_{\text{qper,Ed}}}{W_{y,net}} \qquad \text{Eq. 14}$$

where: $M_{\text{qper,Ed}}$ is 0.4 kNm, being taken from the last row in Table 3. Geometrical property $W_{\text{y,net}}$ = $4.240 \cdot 10^5$ mm$^3$ is taken from the twelve row in Table 1. Using Eq. 14 gives a value of $\sigma_{\text{t,creep,Ed}} = 1.5$ MPa.

For the mode of failure being by tensile creep rupture the ULS check by Eq. 12 is readily satisfied as 1.5/84.8 ≈ 0.02, < 1.0.

*Compressive induced creep rupture*

The second part of the third ULS verification check is for the maximum sustained compressive stress shall, in accordance with the TS, satisfy:

$$\sigma_{\text{c,creep,Ed}} \leq \sigma_{\text{c,creep,Rd}};\ i.e., \frac{\sigma_{\text{c,creep,Ed}}}{\sigma_{\text{c,creep,Rd}}} \leq 1.0 \qquad \text{Eq. 15}$$

where $\sigma_{\text{c,creep,Rd}}$ is the design value of the compressive stress limit for creep rupture, and is determined using the following formula:

$$\sigma_{\text{c,creep,Rd}} = \frac{\eta_c}{\gamma_{\text{M,creep}}} \cdot k_{\text{c,creep}} \cdot f_{\text{i,c,k}} \qquad \text{Eq. 16}$$

For this creep rupture verification check the only changes are on the resistance side, and there are two changes. The first change is that the characteristic strength value is for the compressive strength $f_{\text{x,c,k}}$, and from the seventh row in Table 2 its value is 318 MPa. The The second change is that there is now introduced a strength reduction factor for compressive creep rupture. As a result $k_{\text{c,creep}}$ = 0.3, corresponding to the reduction factor being $0.75 \cdot k_{\text{t,creep}}$. The application of Eq. 16 leads to $\sigma_{\text{c,creep,Rd}}$ = 63.6 MPa. In this verification check the value of $\sigma_{\text{c,creep,Ed}}$ is equal to $\sigma_{\text{t,creep,Ed}}$, and so it is 1.5 MPa.

For the mode of failure being compressive creep rupture the ULS check by Eq. 16 is also readily satisfied as 1.5/63.6 ≈ 0.02, < 1.0.

**SYNTHESIS OF THE RESULTS**

Presented in the third column of Table 5 is a summary for the four ratios from the calculations in checking three ULS modes of failure, defined in the first column, in accordance with the design procedures in CEN/TS 19101. As listed in the second column of the table the checks were conducted using two different member types (see Figures 3 and 4) with the most severe effects of the actions from seven load combination cases for the temporary composite structure at the church of Santa Maria Paganica, in L'Aquila, Italy. Because the ratios range from 0.02 to 0.65 and are < 1.0, it has been established that for these ULS modes of failure the structural design is satisfied in accordance with the TS.

Table 5: Summary of ULS verification checks

| ULS verification | Member | Verification ratio |
|---|---|---|
| Axial compression $(\frac{N_{\text{c,Ed}}}{N_{\text{c,Rd}}})$ | Element 1 Internal column | 0.65 (Eq. 1) |
| Combination of axial tension and bending moment $(\frac{N_{\text{t,Ed}}}{N_{\text{t,Rd}}} + \frac{M_{\text{Ed}}}{M_{\text{Rd1}}})$ | Element 2 Roof beam | 0.63 (Eq. 9) |
| Creep rupture $(\frac{\sigma_{\text{t,creep,Ed}}}{\sigma_{\text{t,creep,Rd}}})$ tensile $(\frac{\sigma_{\text{c,creep,Ed}}}{\sigma_{\text{c,creep,Rd}}})$ compressive | Element 2 Roof beam | 0.02 (Eq. 12)<br>0.02 (Eq. 16) |

## CONCLUDING REMARKS

To support the publication of the European Committee for Standardization (CEN) Technical Specification CEN/TS 19101:2022, "Design of Fibre-Polymer Composite Structures", at set of Worked Examples and a Commentary will be published. This paper provides an overview to the worked examples that scopes the design of a temporary shelter of fibre-polymer composites that was erected in 2011 inside the Santa Maria Paganica church in L'Aquila, Italy, following damaged from a earthquake in 2009. The 3D frame structure for the shelter is constructed using standard pultruded composites profiles. It consists of primary built-up members constructed of four C-profiles connected by means of steel bolting. Two C-profiles have been used for built-up members in the roof structure. Bolted structural joints between the primary members are of gusset plates of bag-moulded glass fibre-reinforced polymer composite. The overview of the worked example scoped in this paper covers the finite element model for SAP2000 structural analyses carried out to determine the effect of actions for seven load cases defined by EN 1990, EN 1991 and the National Annexes for Italy. Internal forces and bending moments have been computed to establish the design envelopes for ULS resistance calculations. To provide a flavour of the ULS design checks that are presented in the worked example this paper determines four verification ratios, in accordance with CEN/TS 19101:2022, for three ULS modes of failure. These ULS modes are for axial compression, combination of axial tension and bending moment, and creep rupture (both for tensile and compressive long-term constant stress). The verification ratios range from 0.02 to 0.65, and because they are < 1.0 the structural design is okay. The worked example to be published will involve verification checks for all the other ULS mode of, including a modal analysis in support of the seismic design of the fibre-polymer composite shelter structure.


## ACKNOWLEDGEMENT

There was no external funding for the project leading to the preparation of the working examples to CEN/TS 19101:2022.


## CONFLICT OF INTEREST

The authors declare that they have no conflicts of interest associated with the work presented in this paper.

## DATA AVAILABILITY

No data was assembled for the production of this paper.

## REFERENCES


CEN/TS 19101: 2022. Design of Fibre-Polymer Composite Structures. European Committee for Standardization (CEN).

EN 1990:2002. Eurocode – Basis of structural design. European Committee for Standardization (CEN).

EN 1991-1-3:2003. Eurocode 1: Actions on structures – Part 1-3: General actions – Snow Loads. European Committee for Standardization (CEN).

EN 1991-1-4:2005. Eurocode 1: Actions on structures – Part 1-3: General actions – Wind Actions. European Committee for Standardization (CEN).

Russo, S. (2012). Experimental and finite element analysis of a very large pultruded FRP structure subjected to free vibration, *Composite Structures*, *94*(3), 1097-1105

Russo, S. (2015), Buckling interactions in columns made by built-up thin, open pultruded FRP shapes, *Journal Reinforced Plastics and Composites*, 88 34:972